Advances in SQUID-detected magnetic resonance force microscopy

Wit, M. de

5

Density and T_1 of surface and bulk spins in diamond in high magnetic field gradients

Small spin ensembles play an important role in many areas of condensed matter physics. Here we present a method to measure spin densities in very dilute spin systems. We report on surface and bulk spin density measurements of diamond, using ultra-sensitive magnetic force microscopy with magnetic field gradients up to 0.5 T/μm. At temperatures between 25 and 800 mK, we measure the shifts in the resonance frequency and quality factor of a cantilever with a micromagnet attached to it. A recently developed theoretical analysis allows us to extract a surface spin density of 0.072 spins/nm^2 and a bulk spin density of 0.4 ppm from this data. In addition, we find an increase of the T_1 time of the surface spins in high magnetic field gradients due to the suppression of spin diffusion. Our technique is applicable to a variety of samples other than diamond, and could be of interest for several research fields where surface, interface or impurity bulk spin densities are an important factor.

This chapter has been published as M. de Wit, G. Welker *et al.*, "Density and T_1 of surface and bulk spins in diamond in high magnetic field gradients", *Phys. Rev. Applied*, Vol. 10, p. 064045, Dec. 2018

5.1 Introduction

Noise coming from paramagnetic impurities is a widespread phenomenon that is relevant to fields ranging from magnetometry to solid-state qubits [132, 133]. An example is NV^- centers in diamond (from now on referred to as "NV-centers"), which have become one of the workhorses in quantum technology. Interaction with paramagnetic impurities is considered one of the main factors that induce decoherence of the NV-center [134]. This decoherence is faster for shallow NV-centers close to the surface and slower for NV-centers in the bulk of the diamond sample, because shallow NV-centers are under the influence of a layer of electron spins at the surface of the diamond [132, 135]. Understanding and potentially eliminating this source of decoherence has been a long-standing goal of the field [136]. Here we present a method to measure the impurity spin density, where the sensor is decoupled from the diamond sample. We use an ultrasoft cantilever with an attached micromagnet that couples to the spins via dipole-dipole interaction. The method is easily transferable to a wide range of samples [51].

Multiple experiments have been conducted to measure the diamond surface impurity spin density and to characterize the properties of this two-dimensional electron spin bath, such as correlation times of the fluctuating spins [135, 137–140]. The measured spin densities differ and range from 0.01 to 0.5 μ_B/nm^2. Most of these experiments were done at room temperature, except for one measurement at 10 K [138]. All mentioned studies used NV-centers to probe the surface electron spin bath. The technological challenge of measuring surface or bulk spin densities on samples other than diamond can be met by use of a scanning NV-center approach [137]. Unfortunately, the detection range of a scanning NV-center approach is limited to a few nanometers. Our method is capable of sensing spins at micrometer distances.

We do our experiments at milliKelvin temperatures, where no surface spin-density measurements on diamond have been performed yet. The low temperature in combination with a high magnetic field gradient allows us to measure with an extremely low force noise [48]. In addition, it allows us to interact with electron spins that can easily be polarized by small magnetic fields and to disregard all physical processes involving phonons. This makes our method suitable for measuring spin densities in very dilute spin systems. In particular, it is of interest for the fields of quantum computation devices [141, 142], magnetometry [143], and magnetic resonance force microscopy (MRFM) [106], as surface and bulk impurity spins play an important role there.

Our group has previously demonstrated surface spin-density measurements of dan-

gling bonds on a silicon oxide surface [51]. Here we present spin-density measurements of paramagnetic impurities on a diamond surface and also expand our method to probe impurity spins in the bulk of the sample. We show that strong magnetic field gradients influence the T_1 relaxation time of the impurity spins and that this effect is an important ingredient to understand the system.

5.2 Methods

5.2.1 Experimental setup

In our experiments we use a commercially available diamond sample with a size of 2.6 x 2.6 x 0.3 mm^3 and that is specified to have less than 1 ppm of nitrogen impurities[1]. One surface is polished twice to a surface roughness R_a <5 nm^2. We clean the diamond subsequently in acetone, 2-propanol, fuming nitric acid, hydrofluoric acid, and water to start the fabrication process with a clean surface and without oxides. On the surface we fabricate a niobium titanium nitride (NbTiN) pickup loop and RF-wire, the latter of which is not used in the present experiment [55]. After fabrication, the sample is exposed to air for several months. Before mounting of the sample, it is ultrasonically cleaned in acetone, and thereafter in 2-propanol to remove organics and dust.

The measurements are performed with a MRFM setup comparable to the one used in earlier experiments [51]. To establish the magnetic interaction, we use a spherical (Nd,Fe)B particle (from now on simply referred to as the "magnet") with a diameter of 2.99 μm. This magnet is glued with platinum by electron-beam-induced deposition (EBID) to the end of an ultrasoft cantilever with a length of 166 μm, width of 5 μm, and thickness of 100 nm [7]. This geometry leads to an intrinsic spring constant $k_0 = 5.0 \times 10^{-5}$ N/m with a corresponding natural frequency of 2850 Hz (see Supplemental Material Fig. 5.7 for the properties of the cantilever measured versus temperature at 5 μm height, far away from the sample). After the magnet is attached, it is placed in an external field of 5 T, leading to a magnetic moment $\boldsymbol{m}$ of 1.5×10^{-11} Am^2 pointing along the direction of movement of the cantilever (Fig. 5.1(a)). The magnetic particle is responsible for the B field, which polarizes the spins in the sample but also creates large magnetic field gradients of up to 0.5 T/μm.

The magnetized cantilever is mounted above the sample and can be moved with

[1] SC Plate CVD, <100>, PL, from Element Six
[2] Second polish: scaife polishing from Stone Perfect

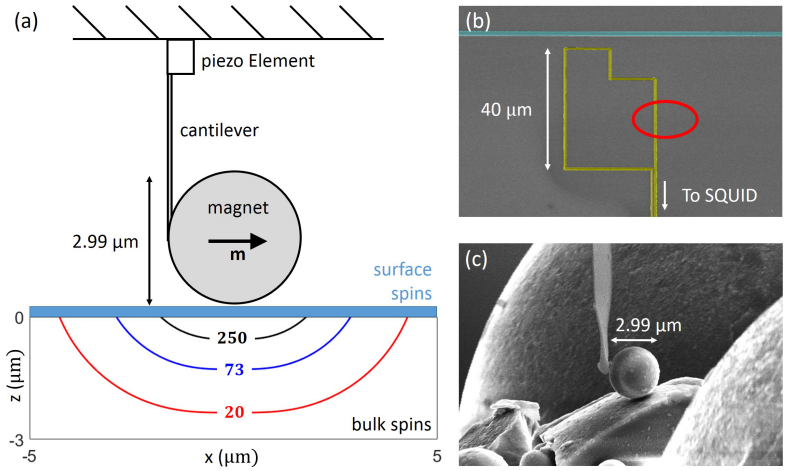

Figure 5.1: (a) Setup: A magnetic particle with a diameter of 2.99 µm attached to the end of a soft MRFM cantilever is positioned above the diamond sample, where it induces a high magnetic field gradient (solid colored lines, unit mT/µm). The bulk of the diamond contains nitrogen impurities with an associated electron spin. On the surface we find an impurity layer containing paramagnetic electron spins, indicated in blue. (b) False-color scanning-electron-microscope image of the nanofabricated structures on top of the diamond sample. The pickup loop used for the read-out of the cantilever is shown in yellow. In blue there is a NbTiN RF wire, which is not used in the current experiment. The measurements described in this work are done at the location marked by the red circle. (c) Scanning-electron-microscope image of the tip of the cantilever and a NdFeB particle after the electron-beam-induced deposition (EBID).

respect to the sample with use of a modified piezoknob-based cryogenic positioning stage[3]. The absolute tip position is measured with three capacitive sensors, while the precise distance between the surface of the magnet and the surface of the diamond is calibrated by gently lowering the magnet until the two touch, using the piezoknobs.

The motion of the cantilever is measured with a SQUID-based read-out [47], where we detect the changing magnetic flux in the pickup loop (yellow in Fig. 5.1(b)) due to the moving magnet. We can determine the linear response of the cantilever by driving a small piezo element at the base of the cantilever. When we sweep the drive frequency and measure the cantilever response using a lock-in amplifier, we obtain the resonance frequency and quality factor by fitting the square of the SQUID output with a Lorentzian, as seen in Fig. 5.2.

The full experimental setup is mounted at the mixing chamber of a cryogen-free

[3]Cryo Positioning Stage - High Resonance (CPSHR), from Janssen Precision Engineering B.V.

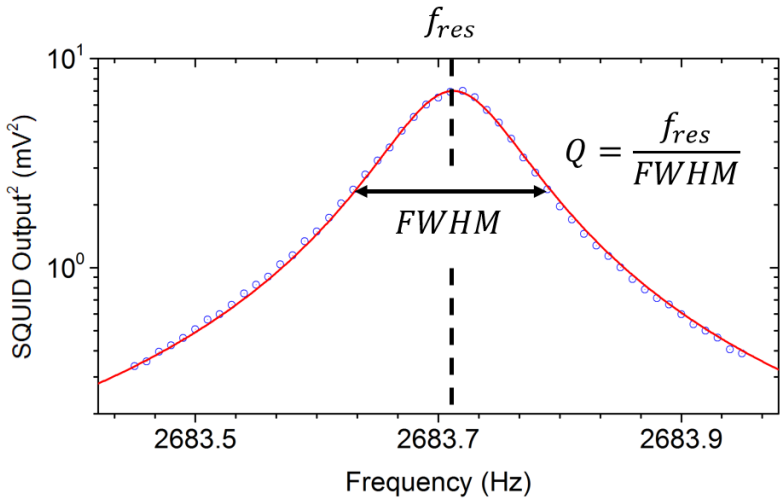

Figure 5.2: Example of a frequency sweep measured at a tip-sample separation of 3.4 µm at a temperature of 25 mK. The resonance frequency and quality factor are obtained by the fitting of the data to a Lorentzian (solid red line).

dilution refrigerator with vibration isolation [77], and with a base temperature of 10 mK. The gold-plated copper sample holder is thermally connected to the mixing chamber with a silver strip. A heater and calibrated low-temperature thermometer are used to control the temperature of the sample holder. Because of the limited thermal conductance between the mixing chamber, the sample holder, and the diamond sample itself, the sample temperature typically saturates at approximately 25 - 30 mK.

5.2.2 Spin-bath - cantilever coupling

When the tip of the cantilever is positioned close to the sample, it couples to the electron spins via the magnetic field that originates from the magnet. The motion of the cantilever changes the direction and strength of this field. The electron spins will follow the varying magnetic field, but with a lag due to their relaxation times T_1 and T_2. This effect will, in return, change the motion of the cantilever. De Voogd *et al.* [52] investigated the complete spin-cantilever system while taking into account the intrinsic damping of the cantilever and the spin-lattice relaxation. They derived an expression for the change of the resonance frequency $\Delta f = f_{\text{res}} - f_0$, where f_{res} is the resonance frequency taking into account the interaction with the spins, and f_0 is the resonance frequency of the cantilever. Only spins with $T_1 \gtrsim 1/\omega_0$, with $\omega_0 = 2\pi f_0$, contribute to the frequency shift. A similar expression is found for the inverse quality

factor $\Delta\frac{1}{Q} = \frac{1}{Q} - \frac{1}{Q_0}$, with Q_0 the cantilever's bare quality factor. The spin-mediated dissipation $1/Q$ is significant only when $T_1 \approx 1/\omega_0$. We now give the expressions for Δf and $\Delta\frac{1}{Q}$ for our specific sample.

In our sample, we expect two main sources for the signal: spins in the bulk and spins on the surface of the diamond. First, we expect a contribution from the free electron spins associated with the nitrogen impurities in the bulk of diamond (P1 and P2 centers). The T_1 relaxation time of the dilute electron spins in the bulk of diamond has been reported to increase to several seconds at low temperatures [144]. Since this means that the spin-lattice relaxation is negligible on timescales comparable to the cantilever period, there is no dissipation path for the cantilever through the spin to the lattice at the cantilever's resonance frequency. Hence, we expect the bulk spin-induced shift of the quality factor to be zero. Taking these assumptions into account, we find the contributions of the spins in the bulk to be

$$\Delta f_{\text{bulk}} = \frac{f_0}{2k_0}\frac{\rho\mu_{\text{B}}^2}{k_{\text{B}}T}\int_V d^3\boldsymbol{r}\ \mathcal{C}(\boldsymbol{r}), \tag{5.1}$$

and

$$\Delta\frac{1}{Q}_{\text{bulk}} = 0, \tag{5.2}$$

where

$$\mathcal{C}(\boldsymbol{r}) = \frac{|\mathbf{B}'_{||\hat{\mathbf{B}}_\mathbf{0}}|^2}{\cosh^2(\frac{\mu_{\text{B}}B_0}{k_{\text{B}}T})}, \tag{5.3}$$

ρ is the bulk spin density, μ_{B} is the Bohr magneton, and T is the temperature of the spin bath. The integral is over the entire volume of the sample.

Since our sample is exposed to air before the experiment, we expect a second contribution from a layer of surface spins that can be expected on any surface that has been exposed to air for extended times [145]. As these are dilute paramagnetic spins, we expect these spins to have T_1 times in the millisecond range. In the case that T_1 is similar to $\frac{1}{\omega_0}$, these spins create an additional dissipation path for the cantilever. Therefore, these spins should cause additional shifts given by

$$\Delta f_{\text{surf}} = \frac{f_0}{2k_0}\frac{\sigma\mu_{\text{B}}^2}{k_{\text{B}}T}\int_S d^2\boldsymbol{r}\ \mathcal{C}(\boldsymbol{r})\frac{(\omega_0 T_1(\boldsymbol{r}))^2}{1+(\omega_0 T_1(\boldsymbol{r}))^2}, \tag{5.4}$$

and

$$\Delta\frac{1}{Q}_{\text{surf}} = \frac{1}{k_0}\frac{\sigma\mu_{\text{B}}^2}{k_{\text{B}}T}\int_S d^2\boldsymbol{r}\ \mathcal{C}(\boldsymbol{r})\frac{\omega_0 T_1(\boldsymbol{r})}{1+(\omega_0 T_1(\boldsymbol{r}))^2}, \tag{5.5}$$

where σ is the surface spin density. We have placed the term containing $\omega_0 T_1$ inside the integral to reflect the fact that T_1 may depend on the magnetic field gradient. The integral is over the entire surface of the sample.

To calculate the expected frequency shift and additional dissipation, accurate values are needed for the magnetic moment and the shape and size of the magnetic field. In our experiment, since the magnetic particle is almost perfectly spherical, we can calculate the field as if it originates from a magnetic dipole. In the coordinate-free form, this is given by [146]

$$\boldsymbol{B}(\boldsymbol{r}) = \frac{\mu_0}{4\pi}\frac{1}{r^3}\left[3\left(\boldsymbol{m}\cdot\hat{\boldsymbol{r}}\right)\hat{\boldsymbol{r}} - \boldsymbol{m}\right], \tag{5.6}$$

where $\mathbf{m}$ is the magnetic moment of the magnet. From this field, we can calculate all relevant derivatives as required for Eq. 5.3.

5.2.3 Spin diffusion in high magnetic field gradients

The theory presented so far describes the spin-cantilever interaction for a constant T_1 of the spins. For most applications (e.g.,in bulk techniques with homogeneous external fields) this is a good approximation. However, this approximation does not hold when dilute spins are placed in large magnetic field gradients, as is the case in our experiment. These gradients can increase the relaxation times by suppressing spin diffusion, a concept first derived by Bloembergen [131]. Spin diffusion in diamond was studied by Cardellino *et al.* [33].

In this model, it is assumed that different spins can have different relaxation times depending on their local environment. This results in the presence of fast-relaxing spins that can rapidly thermalize to the lattice, and slow-relaxing spins that are badly coupled to the lattice. After a perturbation of the thermal equilibrium, relaxation of the polarization of this sample to equilibrium occurs via spin diffusion which couples the slower-relaxing spins to the faster-relaxing spins through flip-flop interaction, reducing the overall relaxation time of the sample.

However, spin diffusion can be suppressed by application of a large magnetic field gradient, which reduces the probability of two spins exchanging energy by introducing a difference in field felt by neighboring spins. An Ansatz for the suppression of the spin diffusion can be obtained by calculation of the normalized overlap integral between the line shapes of two spins [32]:

$$\Phi(\bar{a}G) = \frac{\int F(B')F(B'-\bar{a}G)dB'}{\int F^2(B')dB'}, \tag{5.7}$$

where G is the gradient of the magnetic field strength at the position of the spins, $\bar{a} \simeq 0.5\ \bar{r}$ is the approximate average spacing between spins in the radial direction with $\bar{r}$ the nearest-neighbor distance under the assumption of a cubic lattice, and $F(B)$ is the resonance line shape of the spins. We look at the spacing in the radial direction, since this direction has the largest magnetic field strength gradients, and therefore the highest suppression of spin diffusion. Since we are considering a layer of spins on the surface of the diamond, the total number of spins is too small to measure the actual spectra of the surface spins by bulk techniques such as ESR, so we assume these spins have a Lorentzian profile

$$F(B) = \frac{1}{\pi} \frac{\left(\frac{\Delta B_{\mathrm{dd}}}{2}\right)}{B^2 + \left(\frac{\Delta B_{\mathrm{dd}}}{2}\right)^2}, \tag{5.8}$$

with a linewidth given by [117, p. 128]:

$$\Delta B_{\mathrm{dd}} = 3.8 \mu_0 \gamma_e \hbar / 4\pi \bar{r}^3, \tag{5.9}$$

where $\gamma_e/2\pi = 28.0$ GHz/T is the electron gyromagnetic ratio. Because the convolution of two Lorentzian profiles with width Δ is itself a Lorentzian with width 2Δ, we can evaluate Eq. 5.7, from which we find that

$$\Phi(\bar{a}G) = \frac{1}{1 + (\bar{a}G/\Delta B_{\mathrm{dd}})^2} = \frac{1}{1 + (G/G^*)^2}, \tag{5.10}$$

where $G^* = \Delta B_{\mathrm{dd}}/\bar{a}$ is a measure for the gradient when the quenching becomes significant, from now on called the "critical gradient". In short, it is the gradient for which the difference in the field at neighboring spins becomes larger than the spin linewidth. $\Phi(\bar{a}G)$ can be seen as a flip-flop suppression factor. When $\Phi(\bar{a}G)$ is 0, flip-flops are fully suppressed, and when $\Phi(\bar{a}G)$ approaches 1, spins can exchange energy and flip-flops are possible. Thus, we find that the relaxation time is given by

$$T_1(G) = \left\{ \frac{1}{T_1^{\mathrm{ff}}} \frac{1}{[1 + (G/G^*)^2]} + \frac{1}{T_1^*} \right\}^{-1}, \tag{5.11}$$

where T_1^{ff} is the reduced T_1 time due to flip-flops between neighboring spins and T_1^* is the intrinsic relaxation time of the system when the flip-flops are completely quenched. This is only a heuristic description of the effects of spin diffusion, and does not take into account the direction of the gradient or the effects of the spin-bath polarization on the flip-flop rate.

5.3 Results and discussion

For our experiments, we change the height (distance between the two surfaces of the diamond and the magnet) and vary the temperature from 25 mK to 800 mK. At every height-temperature combination, the resonance frequency and quality factor are measured as described in Sec. 5.2.1.

5.3.1 Frequency shift and dissipation

The results of the measurements of the frequency shift are shown in Fig. 5.3. The solid lines indicate the results of the fits according to Eqs. 5.1 and Eq. 5.4, with the total frequency shift given by $\Delta f = \Delta f_{\text{bulk}} + \Delta f_{\text{surf}}$. We calculate f_0 at each height by extrapolating the measured frequency-shift data to higher temperatures.

The two-dimensional and three-dimensional integrals over $\mathcal{C}(\boldsymbol{r})$ are calculated with the magnetic field distribution defined by Eq. 5.6. As mentioned before, both integrals are calculated over the entire surface and volume, respectively, but they converge within several micrometers from the magnet due to the strong distance-dependence of $\mathcal{C}(\boldsymbol{r})$. The only free parameters remaining in the model are the two spin densities ρ and σ for the bulk and the surface, respectively, and the T_1 time of the surface spins, which for now is fixed at 0.5 ms. As the term $(\omega_0 T_1)^2 / \left[1 + (\omega_0 T_1)^2\right]$ converges to 1 for $\omega_0 T_1 \gg 1$, the effect of the T_1 time on the total frequency shift can be ignored, so the precise value for the T_1 time is important only in the analysis of the temperature-dependent change of the quality factor.

A complication in fitting the values for the two spin densities, is that the functions for Δf_{bulk} and Δf_{surf} are not independent. To determine the precise values, we fix ρ and fit σ as a shared fit parameter over the temperature traces for all heights. Next, we vary ρ to minimize the average fitting error. This method yields global values of ρ = 0.4 ppm, compatible with the specifications of the diamond sample, and $\sigma = 0.072$ spins/nm^2, in line with previously measured surface spin densities [139]. The dashed line in Fig. 5.3 shows the frequency shift due to the bulk spins at a height of 20 nm for this concentration, signifying that even very low spin densities have a substantial effect on the total frequency shift.

The measured changes of the quality factor for each height and temperature are shown in Fig. 5.4. The total value for the inverse quality-factor is given by $\frac{1}{Q} = \frac{1}{Q_0} + \Delta\frac{1}{Q}_{\text{surf}}$, where Q_0 is the quality factor of the resonator without coupling to the

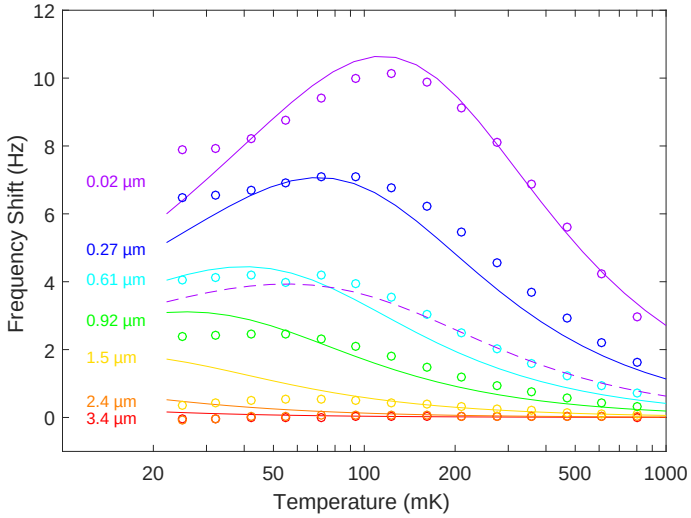

Figure 5.3: Data (circles) and theory (lines) for the frequency shift of the cantilever versus temperature when the cantilever is positioned near the surface of the diamond sample. The dashed line shows the contribution from the bulk spins in the diamond only. The solid lines are calculated with $\sigma = 0.072$ spins/nm^2 and $\rho = 0.40$ ppm.

spin-bath. Q_0 can be obtained by extrapolation of the measured dissipation to high temperatures. For a height of 3.4 μm we find that Q_0 is 24 000, and for a height of 2.4 μm, we find Q_0 to be 18 500. For all smaller heights we fix Q_0 to 18 500. These values are lower than the vacuum quality-factor (at a height of 5 μm, we find Q_0 is 35 000, see Fig. 5.7), and we ascribe this to some other long-range effect (e.g., electrostatic interactions [147, 148]).

To fit the data to Eq. 5.5, we fix the spin densities of both the surface and the bulk to the values obtained from the frequency-shift analysis. Our attempt to fit these data using Eq. 5.5 with a constant T_1 time independent of position did not yield a good match with the data. This is illustrated by the dashed line in Fig. 5.4, which shows the result of the calculation at a height of 20 nm, with $T_1 = 1.3$ ms. A clear deviation between the data and calculated values at low temperatures is visible. Repeating the calculation for each available height separately results in different T_1 times. We find that T_1 increases from 0.4 ms at a large height to 1.3 ms at a small height (see Fig. 5.8 for the fitting results obtained with constant T_1 times). This observation is a strong indication of the suppression of the spin diffusion by the high magnetic field gradient.

We include this effect by inserting Eq. 5.11 into Eq. 5.5, yielding a position-dependent T_1 time bound by T_1^* in the high gradients close to the magnet, and T_1^{ff} for

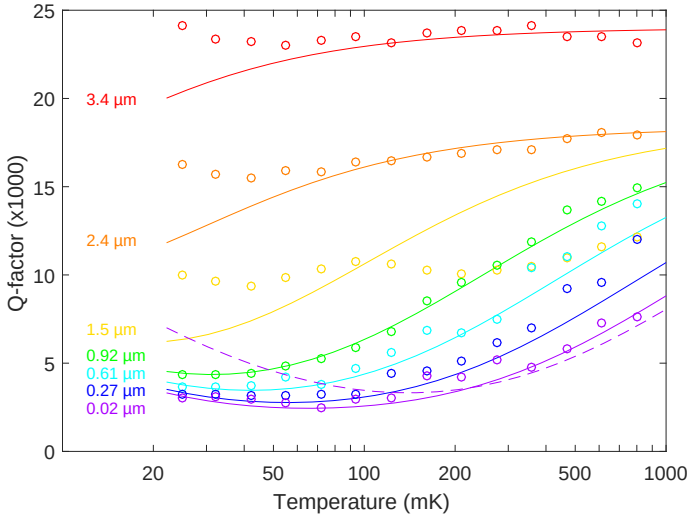

Figure 5.4: Data (circles) and theory (lines) for the change in the quality factor of the cantilever versus temperature when the cantilever is positioned near the surface of the diamond sample. The solid lines are calculated with the spin densities obtained from the frequency data, including the effects of spin diffusion using $T_1^* = 10$ ms and $T_1^{\mathrm{ff}} = 0.45$ ms. The dashed line shows the expected quality factor at a height of 0.02 µm calculated with a constant $T_1 = 1.3$ ms.

spins far away from the magnet. Using the surface spin density $\sigma = 0.072$ spins/nm^2 obtained from the frequency-shift data, we find that in our case $\bar{r} = \sigma^{-1/2} = 3.7$ nm, resulting in a linewidth of $\Delta B_{\mathrm{dd}} = 0.14$ mT according to Eq. 5.9. This leads to a critical gradient $G^* = 73$ mT/µm, a value smaller than the maximum field gradients in our setup as indicated in Fig. 5.1(a). The resulting dependence of the T_1 time on the magnetic field strength gradient is shown in Fig. 5.5.

To obtain reliable values for the relaxation times T_1^{ff} and T_1^*, we use an interesting feature of the coupling between the spins and the magnet. Fig. 5.6 shows the spatial distribution of $\mathcal{C}$ for various temperatures, calculated at a constant tip-sample separation of 20 nm, indicating the position of the spins contributing most to the signal. It is clear that as the temperature of the sample decreases, the average location of contributing spins moves away from the cantilever. This immediately implies that at low temperatures, most of the contributing spins are located in a region with a magnetic field gradient below G^*, which means that spin diffusion is not suppressed, and thus their relaxation time approaches T_1^{ff}. Equivalently, at high temperatures, the spins that contribute the most are close to the magnet in a high magnetic field gradient, meaning flip-flops are quenched and $T_1 \approx T_1^*$. This allows us to fit T_1^{ff} and T_1^* almost independently. The solid lines in Fig. 5.4 show the final calculations including the

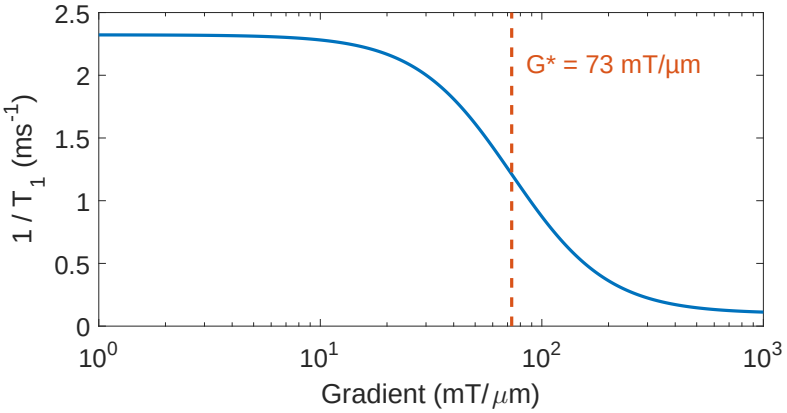

Figure 5.5: Plot of the inverse of the T_1 time calculated from Eq. 5.11, using $G^* = 73$ mT/μm, $T_1^{\text{ff}} = 0.45$ ms, and $T_1^* = 10$ ms.

effects of spin diffusion using $T_1^* = 10$ ms and $T_1^{\text{ff}} = 0.45$ ms.

We select a value of 10 ms for T_1^*. Higher values for T_1^* do not significantly change the dissipation, because T_1^* becomes too far away from the cantilever period. In other words, the dissipation of the cantilever mediated by the spins peaks when T_1 matches the cantilever period, so we are only sensitive to T_1 times of up to several milliseconds. Spins with a T_1 time greater than several milliseconds do not contribute to the enhanced dissipation, but they do change the resonance frequency.

There are still some unexplained features in the data. First, there is a clear difference between data and theory for large tip-surface separations at low temperatures. It seems that the quality factor of the silicon cantilever increases when the temperature decreases (see Supplemental Material Fig. 5.7 for the data showing the increasing Q factor at low temperatures measured at a height of 5 μm), presumably due to the freezing out of the quantum fluctuators on the surface of the silicon beam [149]. Furthermore, the measurements at a height of 1.5 μm also strongly deviate from the fit for both the resonance frequency and the quality factor. This could be because this measurement is performed directly above a superconducting line of the pickup loop, which might lead to a lower density of paramagnetic electron spins on and beneath the superconductor. The low quality factor can then be explained by the increased coupling with the pickup loop, which leads to additional dissipation of the cantilever energy via the inductive coupling to resistive elements. We did not take the data measured at this height into account in our final analysis.

As the measured data as a function of temperature (for each height) show a clear

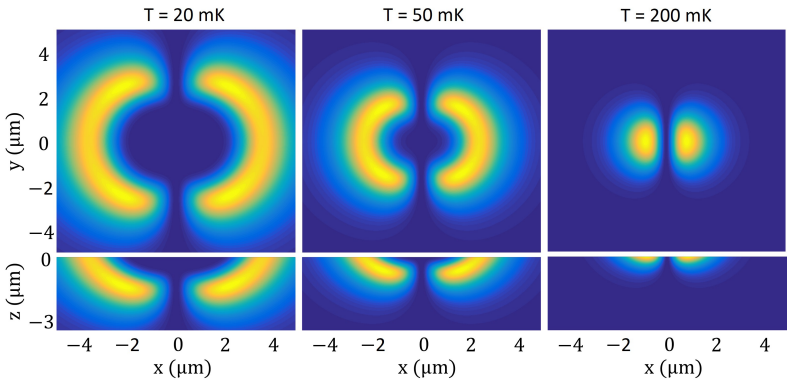

Figure 5.6: Simulation of the relative contribution of spins at different locations, calculated for a tip-sample separation of 20 nm. Yellow indicates regions of maximal coupling, while blue indicates a very low coupling between a spin and the cantilever.

nontrivial curve that matches the magnetic interaction as described by De Voogd et al., we are confident that the observed effects can be ascribed to paramagnetic spins. Other dissipation channels, such as dielectric fluctuations, are estimated to be smaller than what we find. In an improved version of our experiment, we would like to apply an external magnetic field, although this is a large technical challenge because the SQUID detection is very sensitive to noise in the applied external magnetic field.

5.4 Summary and outlook

In conclusion, by using our MRFM setup as an ultra sensitive, long-range magnetic force microscope, we are able to measure the amount of nitrogen impurities in our diamond sample, resulting in a bulk spin density of only 0.4 ppm. This shows that our method allows us to characterize samples containing low spin densities over a field of view of several micrometers. Furthermore, we characterize the paramagnetic electron-like spins on the surface of the diamond, yielding a density of 0.072 spins/nm^2, and T_1 times of several milliseconds, heavily influenced by the presence of spin diffusion. As it is the fluctuation of these spins that is typically held responsible for the reduced performance of a variety of nanodevices such as qubits and superconducting resonators, we believe that our technique offers a useful tool to characterize the properties of the surface spin system and understand the resulting dissipation in these devices.

As the flip-flop interaction between the surface spins on the diamond can be reduced by use of a high gradient, it could be possible to improve the coherence of

various diamond-based devices. The idea of suppressing flip-flop induced spin-bath fluctuations for this purpose has been demonstrated before by increasing the polarization of the spin bath to more than 99% [144]. However, this works only for low temperatures and high magnetic fields. This is not the case for gradient-based quenching of flip-flops. Furthermore, since the required magnitude of the critical gradient depends on the spin density, relatively modest magnetic field strength gradients are required to isolate a single spin from its environment in very pure samples. For example, to suppress spin diffusion in a diamond sample with a nitrogen spin density of 1 ppm, it is sufficient to have a gradient of 1 mT/μm.

A potential near-future application of this technique could be the testing of various sample preparation steps that are typically used to enhance the performance of nanodevices. As an example, we expect that a short chemical wet etch of diamond using hydrofluoric acid should reduce the density of the unpaired spins on the surface, resulting in the case of MRFM in a higher quality factor of the resonator close to the surface and in the case of shallow NV-centers in enhanced correlation times. Our technique would allow us to test the effect of this etch in any intermediate state of the fabrication of one of these devices, allowing better optimization of the fabrication process.

Supplemental material

5.5 Vacuum properties of the cantilever

To exclude the possibility that the mechanical properties of the cantilever might be dependent on the temperature, even at temperature well below 1 K, we have measured the resonance frequency and Q-factor of the cantilever at a height of approximately 5 μm for various temperatures below 1 K. A height of 5 μm is sufficiently far away from the sample that we expect no significant coupling between the spins and the magnetic tip of the cantilever. The results of this measurement are presented in Fig. 5.7. The properties of the cantilever were obtained using the same method as described in Sec. 5.2.1.

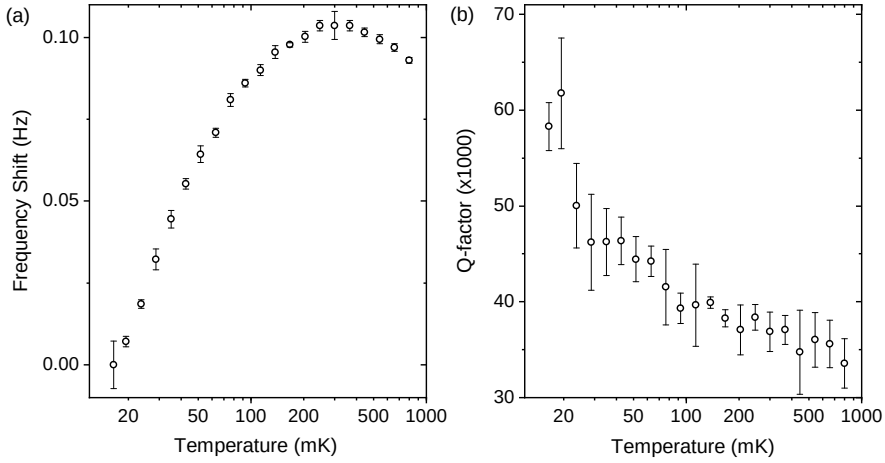

Figure 5.7: Properties of the cantilever measured at a height of 5 μm for various temperatures. The resonance frequency (a) changes by approximately 100 mHz with respect to a reference frequency of 2749.01 Hz. The Q-factor (b) is constant at a value of 35 000 for temperatures above 100 mK, but increases for lower temperatures.

We find that between 16 mK and 800 mK, the resonance frequency shifts by approximately 100 mHz, which is only a fraction of the total frequency shifts measured close to the sample, where spins influence the resonance frequency. We therefore conclude that the mechanical properties of the cantilever, e.g. the Young's modulus and thereby the intrinsic stiffness, do not change significantly within the presented temperature range.

For the Q-factor we find that it is stable at approximately 35 000 for temperatures above 100 mK, and increases to 60 000 for lower temperatures. This rising Q-factor is a possible explanation for the mismatch between the calculation and experiment in the low temperature, large height region of Fig. 5.4, as we pointed out at the end of Sec. 5.3. At small heights, the spin-mediated dissipation is much larger than the intrinsic dissipation in the cantilever, and the changing vacuum Q-factor becomes irrelevant.

5.6 Fits with constant T_1 times

In Sec. 5.3, we note that if we fit the data of Fig. 5.4 using a constant T_1 for each height, we find a clearly increasing T_1 for decreasing height. For completeness, we show the result of this initial analysis in Fig. 5.8, where the circles indicate the data, and the solid lines the theory. As indicated in the main text, a clear deviation at low temperatures is visible. The height of each measurement and the value for T_1 which best fits the data can be found next to the lines. As can be seen, the best fit for a constant T_1 increases from 0.4 ms at a height of 3.4 μm to 1.3 ms at a height of 20 nm. To explain why the T_1 time of a spin close to the magnet is larger than that for a spin far away, we decided to study the effects of the magnetic field gradient on the spin diffusion, the result of which is presented in Sec. 5.3.

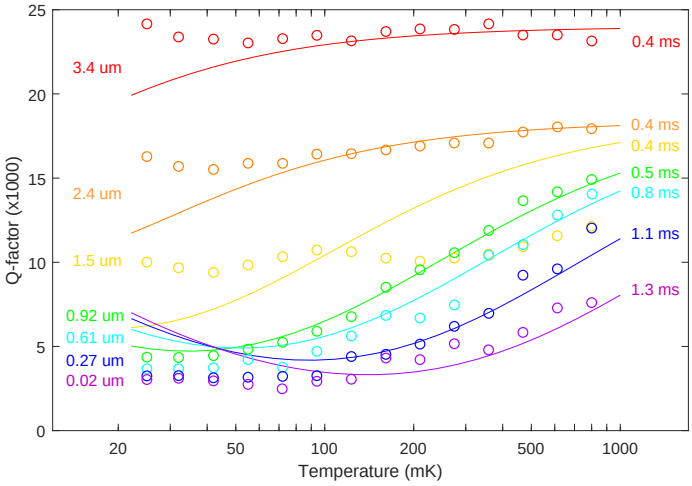

Figure 5.8: Initial analysis of the data from Fig. 5, where we use a constant T_1 for each height. The number on the right of each line shows the best-fit value for T_1, showing a clear trend of increasing T_1 for decreasing height.